EUROGRAPHICS Workshop on ... (200x), pp. 1–16
N.N. and N.N. (Editors)

Extremal Surface Based Projections Converge and Reconstruct with Isotopy

Tamal K. Dey and Samrat Goswami and Jian Sun

Department of Computer Science and Engineering, the Ohio State University, USA. *{tamaldey,goswami,sunjia}@cse.ohio-state.edu}*

Abstract

Many real world applications need to model a smooth surface from a noisy point sample. In order to eliminate unnecessary undulations on the output surface, it is necessary to project the points on a nearby smooth surface and then approximate the smooth surface with a surface reconstruction algorithm. Moving Least Square (MLS) surfaces in the family of extremal surfaces have been shown to be useful as projection targets. However, it is unknown if the extremal surface based projection procedure converges and if the target extremal surface is isotopic to the original sampled surface. We prove these two facts. The success of the entire projection method depends on the quality of the estimated normals at the sample points. We suggest an algorithm to estimate the normals from the noisy samples which can be of independent interest for other applications. We also present some experimental results.

Categories and Subject Descriptors (according to ACM CCS): I.3.3 [Computer Graphics]: Line and Curve Generation

1. Introduction

The importance of computing a surface from a set of unorganized points cannot be over emphasized in a number of applications of computer graphics, vision, geometric modeling and others. The point sets, often derived with a scanning process, are likely to be "noisy". A reconstructed surface interpolating these or a subset of these points may be unnecessarily undulated even though computed with a provable algorithm [DG04] or an effective practical algorithm [KSO04] (Figure 5). A solution to this problem is to define a smooth surface based on the given point set and then generate points on that smooth surface for reconstruction. This is a dominant approach in computer graphics and vision.

1.1. Background and results

Different types of smooth surfaces have been proposed for reconstruction [ABCO*01, JCCCM*01, OBA*03]. Among them the Moving Least Squares (MLS) surfaces, originally proposed by Levin [Lev98] and adopted by Alexa et al. for reconstruction [ABCO*01] have been widely used for modeling and rendering [AA03, MVF03, PKKG03]. This surface is the basis for the popular open source software PointShop 3D [ZPKG02]. The effectiveness of these MLS surfaces and their variants on real world scanned data has made them popular. These surfaces lend to an elegant projection method by which points can be projected onto the surface.

Recently two significant progresses were made to broaden the understanding of the MLS surfaces. First, Amenta and Kil [AK04] pointed out that the MLS surfaces belong to a special class of surfaces called *extremal surfaces*. They showed that the points on these extremal surfaces can also be computed by an elegant projection method though the convergence of the method remained unresolved. Second, Kolluri [Kol05] showed an approach to prove geometric and topological guarantees for reconstruction with a specific type of implicit surface. This implicit surface does not belong to the class of MLS surfaces we are considering. We use the insights from these two sources to prove that the projection procedure of Amenta and Kil [AK04] indeed converges to an extremal surface that is isotopic and geometrically close to the surface from which the input points are sampled.

The projection procedure requires a normal field which can be derived from the estimated normals at the input

points. We derive a method from an earlier work [DG04] to estimate the normals with certain guarantees and use them for projecting points onto the extremal surface.

1.2. Extremal surface

Levin [Lev98] pioneered the MLS surface which is defined as the stationary set of a map f, i.e., the points x with $f(x) = x$. For a given point set $P \subset \mathbb{R}^3$, the map f is defined via an energy function e as follows. Given a direction $m \in \mathbb{R}^3$ and a real $t \in \mathbb{R}$, $e(m,t)$ is the sum of the weighted distances of all points in P from a plane with normal m and passing through the point $y = x + tm$. The nearest point to x where e is minimized over all directions and all reals is $f(x)$. Amenta and Kil [AK04] observed that the minimization procedure can be decomposed into two steps by first estimating the optimum direction at x and then carrying out a second optimization along that direction to reach the minimum. This interpretation allows the first optimization step to be replaced by other pre-computed normal vector field n over $\mathbb{R}^3$. Then, the MLS surface becomes precisely the set of points x where the normal vector $n(x)$ is orthogonal to the gradient of the energy function e. These type of surfaces are called *extremal*. Below we review this construction in details.

Let v_p denote the normal vector assigned to a point in P. Define a normal vector field as the normalized weighted average of the normals at the sample points, i.e.,

$$n(x) = \frac{\sum_{p\in P} w_p(x) v_p}{\| \sum_{p\in P} w_p(x) v_p \|}$$

where w_p is a Gaussian with width $h_n > 0$, i.e., $w_p(x) = e^{-\frac{\|x-p\|^2}{h_n^2}}$. The line passing through x in the direction of $n(x)$ is denoted $\ell_{x,n(x)}$.

Let $\pi_p(x,u)$ be the projection of a vector $x - p$ on the vector u, i.e., $\pi_p(x,u) = (x-p)^T u$. In addition, let $\pi_p(x) = \pi_p(x, n(x))$.

Define an energy function $\mathcal{E}: \mathbb{R}^3 \times \mathbb{R}^3 \to \mathbb{R}$ where for any point $y \in \mathbb{R}^3$ and a normal $m \in \mathbb{R}^3$

$$\mathcal{E}(y,m) = \sum_{p\in P} \pi_p^2(y,m)\theta(p,y).$$

The function θ is a weighting function. Similar to the normal field construction, the weighting function $\theta(p,y)$ is taken as a Gaussian: $\theta(p,y) = e^{-\frac{\|y-p\|^2}{h_e^2}}$ where $h_e > 0$. For a point x let x_m be the extremum of $\mathcal{E}(y, n(x))$ over the set $y \in \ell_{x,n(x)}$, i.e.,

$$n(x)^T \left(\frac{\partial \mathcal{E}(y, n(x))}{\partial y}\Big|_{x_m}\right) = 0. \tag{1.1}$$

The point x is a stationary point if $x = x_m$. One can observe that the set of stationary points is actually the 0-level set of the implicit function

$$g(x) = n(x)^T \left(\frac{\partial \mathcal{E}(y, n(x))}{\partial y}\Big|_{x}\right).$$

The set $g^{-1}(0)$ is an extremal surface since the normal vectors of n are orthogonal to the gradient field of the energy function $\mathcal{E}$ precisely at the points of $g^{-1}(0)$. Amenta and Kil [AK04] proposed the following procedure to project a point x onto the surface $g^{-1}(0)$. Starting from x search for the nearest extremum x_m of $\mathcal{E}$ over the set $y \in \ell_{x,n(x)}$. Once x_m is found, take it as a new x and search for its x_m until a stationary point is reached. The question of the convergence of this iterative projection remained unresolved. For reconstruction of Σ, the points of P are projected onto $g^{-1}(0)$. So, it is important to show that the subset of $g^{-1}(0)$ lying close to Σ is topologically equivalent to Σ. If the assigned normal vectors to the sample points approximate the true normals of Σ closely we can show the following.

(i) The projection procedure indeed converges to a point of $g^{-1}(0)$ when the point set P is sufficiently dense and the initial point x is chosen sufficiently close to Σ.
(ii) The subset W of $g^{-1}(0)$ onto which points are projected is indeed homeomorphic to Σ and even a stronger statement holds. The surfaces W and Σ are isotopic, i.e., one can be continuously deformed to the other always maintaining a homeomorphism between them.

As indicated above, the success of the entire projection procedure depends on the quality of the assigned normals. We use a Delaunay algorithm to estimate the normals at the sample points.

It is appropriate to mention that the above guarantees are proved assuming extremely dense sampling. Also, the domain of convergence turns out to be extremely small. We believe that this is only an artifact of our proofs. Perhaps a more careful and most likely more complicated analysis can improve these relevant numbers.

2. Preliminaries

2.1. Surface and thickening

Let $\Sigma \subset \mathbb{R}^3$ be a smooth, compact surface without boundary. For simplicity assume that Σ has a single connected component. Let Ω_I and Ω_O denote the bounded and unbounded components of $\mathbb{R}^3 \setminus \Sigma$ respectively. For a point $z \in \Sigma$, let $\tilde{n}_z$ denote the oriented normal of Σ at z where $\tilde{n}_z$ points locally toward the unbounded component Ω_O.

For a point $x \in \mathbb{R}^3$ and a set $X \subset \mathbb{R}^3$, let $d(x,X)$ denote the distance of x to X, i.e., $d(x,X) = \inf_{y\in X} \|x-y\|$. The medial axis M of Σ is the closure of the set $Y \subset \mathbb{R}^3$ where for each $y \in Y$ the distance $d(y,\Sigma)$ is realized by two or more points. In other words, M is the locus of the centers of the maximal balls whose interiors are empty of any point from Σ.

Let $\nu : \mathbb{R}^3 \to \Sigma$ be the map where $\nu(x)$ is the closest point

of $x \in \mathbb{R}^3$ in Σ. It is known that ν is well defined if its domain avoids M which will be the case for our use of ν. Denote $\tilde{x} = \nu(x)$. Let $\phi(x)$ denote the signed distance of a point x to Σ, i.e., $\phi(x) = (x-\tilde{x})^T \tilde{n}_{\tilde{x}}$. For a real $\delta > 0$ and an integer $k > 0$, define a family of offset surfaces $\Sigma_{+k\delta}$ and $\Sigma_{-k\delta}$ where

$$\Sigma_{+k\delta} = \{x \in \mathbb{R}^3 \mid \phi(x) = k\delta\}$$

$$\Sigma_{-k\delta} = \{x \in \mathbb{R}^3 \mid \phi(x) = -k\delta\}.$$

Let $k\delta\Sigma$ be the region between $\Sigma_{-k\delta}$ and $\Sigma_{+k\delta}$, i.e.,

$$k\delta\Sigma = \{x \in \mathbb{R}^3 \mid -k\delta \le \phi(x) \le k\delta\}.$$

We use $k = 1, 2$ throughout the paper, see Figure 1.

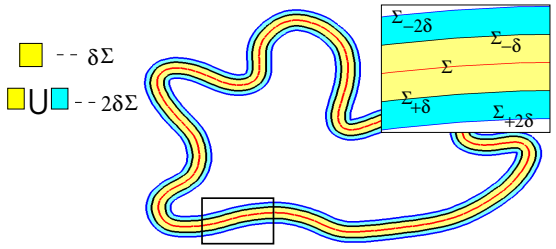

Figure 1: *The set* $\delta\Sigma$ *and* $2\delta\Sigma$.

In what follows we denote the 2-norm of a vector v with $\|v\|$ and the spectral norm of a matrix M with $\|M\|$, which is the square root of the maximum eigenvalue of $M^T M$. A ball with the center x and radius r is denoted as $B(x,r)$. Denote $S(x,r)$ to be the boundary of $B(x,r)$.

2.2. Sampling

The local feature size at a point $x \in \Sigma$ is defined as $d(x,M)$. Sampling density based on the local feature size called ε-sampling has been used for proving the correctness of several surface reconstruction algorithms [AB99, ACDL02, BC00]. For this work we assume uniform sampling density as was used by Kolluri [Kol05] for smooth surface reconstruction. Assume that the smallest local feature size of Σ is 1. We say $P \subset \mathbb{R}^3$ is a uniform $(\varepsilon, \alpha)-$sample of the surface Σ if the following sampling conditions hold.

(i) The distance from each point $x \in \Sigma$ to its closest sample is less than ε.
(ii) The distance from each sample $p \in P$ to its closest point $\tilde{p}$ on Σ is less than ε^2.
(iii) The number of the sample points inside any ball of radius ε is less than a small number α.
(iv) Each point p is equipped with a normal v_p where the angle between v_p and the normal $\tilde{n}_{\tilde{p}}$ at its closest point $\tilde{p}$ on Σ is less than ε.

Let $\mathbb{S}_x(w,r)$ be the region between $S(x,w)$ and $S(x,w+r)$. One can decompose the entire space outside $B(x,r)$ using $\mathbb{S}_x(w_i,r)$ where $w_i = ir$ for $i = 1, 2...$

If P is an (ε, α)-sample, Kolluri [Kol05] proved the following two lemmas.

Lemma 1 For a point $z \in \Sigma$, let $\mathcal{P}_+$ and $\mathcal{P}_-$ be two planes perpendicular to $\tilde{n}_z$ and at a distance of $\frac{(r+\varepsilon^2)^2}{2} + \varepsilon^2$ from z, then any sample point inside $B(z,r)$ should be inside the region bounded by the planes $\mathcal{P}_+$ and $\mathcal{P}_-$.

Lemma 2 The number of sample points inside $\mathbb{S}_x(w,r)$ is less than

$$\frac{C_1}{2\varepsilon^2}(w^2 + wr + r^2)$$

where $C_1 = 288\sqrt{3}\pi\alpha$.

2.3. Normal lemmas

We derive several properties of the normal field which become useful for the convergence and isotopy proofs. The results are important by their own rights. A smooth normal vector field that interpolates a set of given normal vectors is often used in graphics literature [GM97]. The guarantees proved here may also be useful in these contexts.

Our sampling condition implies that two nearby sample points have similar assigned normal vectors.

Lemma 3 Let p_i and p_j be any two sample points inside $B(x,r)$ for a point $x \in 2\delta\Sigma$. If $r + \varepsilon^2 + 2\delta < \frac{1}{3}$, then,

$$\angle v_{p_i}, v_{p_j} \le 2\left(\frac{r+\varepsilon^2+2\delta}{1-3(r+\varepsilon^2+2\delta)} + \varepsilon\right)$$

Proof $d(\tilde{x}, \tilde{p}_i) \le d(\tilde{x}, x) + d(x, p_i) + d(p_i, \tilde{p}_i) \le 2\delta + r + \varepsilon^2$. So, $\angle \tilde{n}_{\tilde{x}}, \tilde{n}_{\tilde{p}_i} \le \frac{r+\varepsilon^2+2\delta}{1-3(r+\varepsilon^2+2\delta)}$ by a result of Amenta and Bern [AB99]. By the sampling condition (iv), $\angle \tilde{n}_{\tilde{x}}, v_{p_i} \le \frac{r+\varepsilon^2+2\delta}{1-3(r+\varepsilon^2+2\delta)} + \varepsilon$. Similarly, we could have a same upper bound for $\angle \tilde{n}_{\tilde{x}}, v_{p_j}$. □

Let $A = [v_p]_{p \in P}$ be the row vector of the equipped normals of all sample points in P and $w(x) = [w_p(x)]^T_{p \in P}$ be the column vector of weights of all sample points for x. Then we can write

$$n(x) = \frac{Aw(x)}{\|Aw(x)\|}. \tag{2.2}$$

Let $J(n(x))$ be the 3×3 Jacobian matrix of the vector field n at x, i.e., $J(n(x)) = \{\frac{\partial}{\partial x_i} n_j(x)\}$, and $w'(x)$ be the $n \times 3$ matrix where $w'(x) = [\frac{d}{dx} w_p(x)]^T_{p \in P}$. Then

$$J(n(x)) = \left(1 - \frac{(Aw(x))(Aw(x))^T}{(Aw(x))^T (Aw(x))}\right) \frac{Aw'(x)}{\|Aw(x)\|} \tag{2.3}$$

Lemma 4 For any point $x \in \mathbb{R}^3$, and any point $p \in P$

(i) $n^T(x) J(n(x)) = 0$,
(ii) $n^T(x) J(n(x))(x-p) = 0$.

Proof Follows from equations 2.2 and 2.3. □

The proofs of the next three lemmas are placed in the appendix for space limitation. The next lemma says that $n(x)$ and the normal to Σ at the closest point of x are very similar when x is close to Σ.

Lemma 5 If $h_n \leq 0.01$, $10\varepsilon \leq h_n \leq 1000\varepsilon$ and $\alpha \leq 10$, then for any point $x \in 2\delta\Sigma$ with $\delta = 0.08\varepsilon$,

$$\angle n(x), \tilde{n}_{\tilde{x}} \leq C_2 + 216 C_1 e^{-36} \frac{h_n^2}{\varepsilon^2}.$$

where $C_2 = \frac{6h_n+\varepsilon^2+2\delta}{1-3(6h_n+\varepsilon^2+2\delta)} + \varepsilon$.

Notice the requirement of h_n in terms of ε. It cannot be too big or too small compared to ε.

Lemma 6 If $h_n \leq 0.01$, $10\varepsilon \leq h_n \leq 1000\varepsilon$ and $\alpha \leq 10$, then for any point $x \in 2\delta\Sigma$ with $\delta = 0.08\varepsilon$,

$$\|J(n(x))\| \leq \frac{24C_3}{h_n}$$

where

$$C_3 = \frac{\left(1 + 108C_1 \frac{h_n^2}{\varepsilon^2} e^{-36}\right)}{\left((1-4C_2^2)^{\frac{1}{4}} - 108C_1 \frac{h_n^2}{\varepsilon^2} e^{-36}\right)}.$$

Intuitively, $\|J(n(x)\|$ measures the rate of variation of $n(x)$. Because of the Gaussian weights, bigger h_n makes the normal vector field flatter. This is reflected in Lemma 6 which says that the order of $\|J(n(x))\|$ is h_n^{-1}.

The following lemma accounts for the variation of the normal field along $\ell_{x,n(x)}$, the line through x along $n(x)$.

Lemma 7 If $0.001 \leq h_n \leq 0.01$, $10\varepsilon \leq h_n \leq 100\varepsilon$ and $\alpha \leq 10$, then for any two points $x, y \in \delta\Sigma$ and $y \in \ell_{x,n(x)}$ where $\|x-y\| \leq 2\delta$ and $\delta = 0.08\varepsilon$, we have

$$\angle n(x), n(y) \leq \frac{75\|x-y\|}{\sqrt{h_n}}.$$

Observe that the variation of the normal vector field along the normal direction of a point inside $2\delta\Sigma$ is of the order of $h_n^{-\frac{1}{2}}$ instead of h_n^{-1}, which means the normal vector field is flatter along the normal direction.

3. Convergence

We prove the convergence of the projection procedure by showing that each time we get to a new point x, the absolute value $|g(x)|$ is decreased by a constant factor.

3.1. Observations

First, we make some observations whose proofs are given in the appendix. Figure 2 aids understanding the statements of the observations. The point x is on $\Sigma_{+\delta}$; $\mathcal{P}_-$ and $\mathcal{P}_+$ are the planes with normal $\tilde{n}_{\tilde{x}}$ and $(r+\delta)^2+\varepsilon^2$ distance away from $\tilde{x}$. All the sample points inside $B(x,r)$ are also inside $B(\tilde{x}, r+\delta)$ and between the planes $\mathcal{P}_-$ and $\mathcal{P}_+$ from Lemma 1.

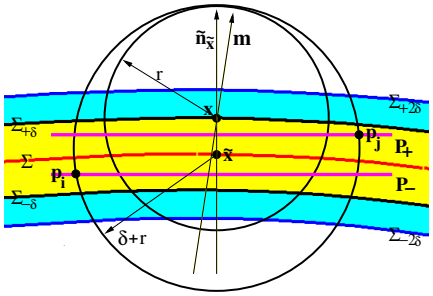

Figure 2: *Observation*

Observation 1 For any point $x \in \delta\Sigma$ and any sample points p_i, p_j inside $B(x,r)$ if $\angle m, \tilde{n}_{\tilde{x}} < \frac{\pi}{2} - asin\frac{(r+\delta)^2+\varepsilon^2}{r+\delta}$ for a unit vector m, then

$$|m^T(p_j - p_i)| \leq 2((r+\delta)^2 + \varepsilon^2 + (r+\delta)\angle m, \tilde{n}_{\tilde{x}}).$$

Observation 2 For any point $x \in \delta\Sigma$ and any sample point $p \in B(x,r)$, if $\angle m, \tilde{n}_{\tilde{x}} < \frac{\pi}{2} - asin\frac{\delta+(r+\delta)^2+\varepsilon^2}{r+\delta}$ for a unit vector m, then

$$|\pi_p(x,m)| \leq \delta + (r+\delta)^2 + \varepsilon^2 + d(p, \ell_{\tilde{x},\tilde{n}_{\tilde{x}}})\angle m, \tilde{n}_{\tilde{x}}.$$

A similar upper bound for $|\pi_p(x,m)|$ when $x \in 2\delta\Sigma$ can be obtained by simply replacing δ with 2δ.

Observation 3 For any $p \in P$ inside $B(x,r)$ if $\angle m, \tilde{n}_{\tilde{x}} < atan\frac{\delta-(r+\delta)^2-\varepsilon^2}{r+\delta}$ for a unit vector m, then

$$\begin{aligned} \pi_p(x,m) &\geq E \text{ when } x \in (2\delta\Sigma - \delta\Sigma) \cap \Omega_O \\ &\leq E \text{ when } x \in (2\delta\Sigma - \delta\Sigma) \cap \Omega_I \end{aligned}$$

where

$$E = (\delta - (r+\delta)^2 - \varepsilon^2)(1 - \angle m, \tilde{n}_{\tilde{x}}) - d(p, \ell_{\tilde{x},\tilde{n}_{\tilde{x}}})\angle m, \tilde{n}_{\tilde{x}}.$$

The proof for convergence as well as the proof for the isotopy in the next section use the following setting: $\alpha = 5$ and $\varepsilon = 10^{-5}$, $h_n = 100\varepsilon$, $h_e = 1.6\varepsilon$ and $\delta = 0.08\varepsilon$. Notice that these values satisfy the conditions of the normal lemmas in the previous section. The proofs can also accommodate other values as long as the conditions for the normal lemmas are satisfied with sufficiently small ε.

With the chosen values, we have $\angle n(x), \tilde{n}_{\tilde{x}} < 6.5 \times 10^{-3}$ for $x \in 2\delta\Sigma$ from Lemma 5. Hence Observation 2 and Observation 3 give the following results:

(i) $|\pi_p(x)| < 0.135 h_e$ for any point $x \in 2\delta\Sigma$ and any sample point $p \in B(x, 5h_e)$.
(ii) $|\pi_p(x)| < 0.085 h_e$ for any point $x \in \delta\Sigma$ and any sample point $p \in B(x, 5h_e)$.
(iii) $\pi_p(x) > 0$ for any point $x \in (2\delta\Sigma - \delta\Sigma) \cap \Omega_O$ and any sample point $p \in B(x, 5h_e)$.
(iv) $\pi_p(x) > 0.045 h_e$ for any point $x \in (2\delta\Sigma - \delta\Sigma) \cap \Omega_O$ and any sample point $p \in B(\tilde{x}, \varepsilon)$.

3.2. Function $\mathcal{G}$

To prove the convergence of the projection procedure, we define a function $\mathcal{G}$ where

$$\mathcal{G}(y,m) = m^T\big(\frac{\partial \mathcal{E}(y,m)}{\partial y}\big)$$

for any point $y \in \mathbb{R}^3$ and a vector $m \in \mathbb{R}^3$. If x_m is a local extremum of $\mathcal{E}(y,n(x))$ over the set $y \in \ell_{x,n(x)}$, from equation 1.1 we have

$$\mathcal{G}(x_m, n(x)) = 0. \tag{3.4}$$

In addition,

$$\mathcal{G}(x, n(x)) = g(x). \tag{3.5}$$

We write $\mathcal{G}(y,m) = \sum_{p\in P}\mathcal{G}_p(y,m)$ where

$$\mathcal{G}_p(y,m) = e^{-\frac{\|y-p\|^2}{h_e^2}}\pi_p(y,m)\big(1-\frac{\pi_p^2(y,m)}{h_e^2}\big). \tag{3.6}$$

Here we drop a factor of 2 since it does not affect the sign of $\mathcal{G}(y,m)$ and the direction of its partial derivatives. Let $\bigtriangledown_y\mathcal{G}_p(y,m)$ and $\bigtriangledown_m\mathcal{G}_p(y,m)$ be the partial derivatives of $\mathcal{G}_p(y,m)$ with respect to y and m respectively. One can verify

$$\begin{aligned}\bigtriangledown_y\mathcal{G}_p(y,m) = e^{-\frac{\|y-p\|^2}{h_e^2}}\big[\big(1-\frac{3\pi_p^2(y,m)}{h_e^2}\big)m \\ +2\big(\frac{\pi_p^3(y,m)}{h_e^4}-\frac{\pi_p(y,m)}{h_e^2}\big)(y-p)\big]\end{aligned} \tag{3.7}$$

and

$$\bigtriangledown_m\mathcal{G}_p(y,m) = e^{-\frac{\|y-p\|^2}{h_e^2}}\big(1-\frac{3\pi_p^2(y,m)}{h_e^2}\big)(y-p). \tag{3.8}$$

The proof for convergence uses the observation that the sample points outside $B(y,5h_e)$ have little effect on $\mathcal{G}(y,m)$ since the weight of a sample point outside $B(y,5h_e)$ is less than $e^{-25} \approx 1.38\times10^{-11}$, a very small value. This observation leads us to decompose $\mathcal{G}(y,m)$ as

$$\mathcal{G}(y,m) = \sum_{p\in B(y,5h_e)}\mathcal{G}_p(y,m) + \sum_{p\notin B(y,5h_e)}\mathcal{G}_p(y,m)$$

We use this decomposition in the proofs to follow.

3.3. Monotonicity of $\mathcal{G}$

Let x be any point in $\delta\Sigma$. Let a and b be the closest points to $\tilde{x}$ where $\ell_{\tilde{x},\tilde{n}_{\tilde{x}}}$ intersects $\Sigma_{+\delta}$ and $\Sigma_{-\delta}$ respectively. Let $\mathcal{P}_+$ and $\mathcal{P}_-$ be the planes with the normal $n(x)$ and passing through a and b respectively, see Figure 3. Further, let $\ell_{x,n(x)}$ intersect $\mathcal{P}_+$ and $\mathcal{P}_-$ at x_+ and x_- respectively. One can verify that $\|y-\tilde{x}\| \le \delta$ for any point y on the segment from x_- to x_+, which means $y \in \delta\Sigma$, and $\|x_+ - x_-\| \le 2\delta$.

The implication of the next two lemmas is that the function $\mathcal{G}$ is monotonic and crosses zero only once along $\ell_{x,n(x)}$ within a small neighborhood of Σ. The proofs of these lemmas appear in the appendix.

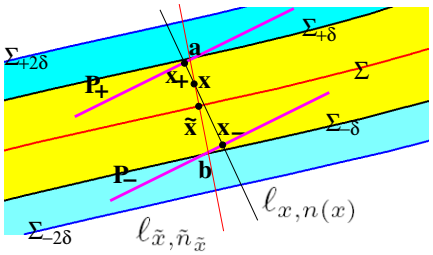

Figure 3: *The planes $\mathcal{P}_+$ and $\mathcal{P}_-$ and the points x_+ and x_-.*

Lemma 8 For any point y on the segment from $x_- - 2\delta n(x)$ to $x_+ + 2\delta n(x)$,

$$n(x)^T\bigtriangledown_y\mathcal{G}(y,n(x)) > 0$$

Lemma 9 $\mathcal{G}(x_+,n(x)) > 0$ and $\mathcal{G}(x_-,n(x)) < 0$.

Lemma 8 and 9 give the following result which says that the point x_m generated (iteratively) in the projection procedure remain within a small thickening of Σ.

Lemma 10 For a point $x \in \delta\Sigma$, if x_m is its nearest local extremum of $\mathcal{E}(y,n(x))$ over the set $y \in \ell_{x,n(x)}$, then $x_m \in \delta\Sigma$ and $\|x - x_m\| \le 2\delta$.

Proof We know from Lemma 8 that $\mathcal{G}(y,n(x))$ is monotonic along the segment from $x_- - 2\delta n(x)$ to $x_+ + 2\delta n(x)$. By Lemma 9, there is a unique 0-crossing point on the segment from x_- to x_+, which actually is a local minimum point of $\mathcal{E}(y,n(x))$ over the set $y \in \ell_{x,n(x)}$, see Figure 3. The 0-crossing point is the nearest local extremum of $\mathcal{E}(y,n(x))$ over the set $y \in \ell_{x,n(x)}$ to x since $\|x_+ - x_-\| < 2\delta$. We know any point on the segment from x_- to x_+ is inside $\delta\Sigma$, so is x_m. We have $\|x - x_m\| \le 2\delta$ since x is also on the segment from x_- to x_+. □

Now we have all ingredients to prove the convergence of the projection procedure.

3.4. Convergence theorem

Theorem 1 For a point $x \in \delta\Sigma$ and $g(x) \neq 0$, if x_m is its nearest local extremum of $\mathcal{E}(y,n(x))$ over the set $y \in \ell_{x,n(x)}$, then

$$\frac{|g(x_m)|}{|g(x)|} < \frac{1}{2}.$$

Proof Due to equations 3.4 and 3.5 it is sufficient to prove

$$\frac{|\mathcal{G}(x_m,n(x_m)) - \mathcal{G}(x_m,n(x))|}{|\mathcal{G}(x,n(x)) - \mathcal{G}(x_m,n(x))|} < \frac{1}{2}.$$

Let $u = \frac{x_m - x}{\|x_m - x\|}$, which is either $n(x)$ or $-n(x)$ since x_m is on $\ell_{x,n(x)}$. Let $t \in (0, \|x_m - x\|)$ and $v(\theta)$ be a unit vector between $n(x)$ and $n(x_m)$ forming an angle θ with $n(x)$. we have

$dv(\theta) = v_\perp(\theta)d\theta$, where $v_\perp(\theta)$ is a unit vector perpendicular to $v(\theta)$. Based on the above notations, equation 3.7 gives

$$\begin{aligned}
&\mathcal{G}_p(x_m, n(x)) - \mathcal{G}_p(x, n(x)) = \\
&\int_0^{\|x_m - x\|} (\nabla_y \mathcal{G}_p(x + tu, n(x)))^T u dt = \\
&\pm \int_0^{\|x_m - x\|} e^{-\frac{\|x+tu-p\|^2}{h_e^2}} \big(1 - 5\frac{\pi_p^2(x+tu, n(x))}{h_e^2} \\
&+ 2\frac{\pi_p^4(x+tu, n(x))}{h_e^4}\big) dt.
\end{aligned} \tag{3.9}$$

If $u = n(x)$, we have the positive sign. Otherwise, we have the negative sign. In addition, equation 3.8 gives

$$\begin{aligned}
&\mathcal{G}_p(x_m, n(x_m)) - \mathcal{G}_p(x_m, n(x)) = \\
&\int_0^{\angle n(x), n(x_m)} (\nabla_m \mathcal{G}_p(x_m, v(\theta)))^T v_\perp(\theta) d\theta = \\
&\int_0^{\angle n(x), n(x_m)} e^{-\frac{\|x_m - p\|^2}{h_e^2}} \big(1 - \frac{3\pi_p^3(x_m, v(\theta))}{h_e^2}\big) \\
&(x_m - p)^T v_\perp(\theta) d\theta.
\end{aligned} \tag{3.10}$$

Also, $\|x_m - x\| \le 2\delta$ and the segment from x to x_m is inside $\delta\Sigma$ from Lemma 10. Hence $\angle n(x), n(x+tu) < 75\frac{t}{\sqrt{h_n}}$ from Lemma 7. In particular,

$$\angle n(x), n(x_m) < 75\frac{\|x_m - x\|}{\sqrt{h_n}} \tag{3.11}$$

which is less than 3.80×10^{-3}.
First consider any sample points p outside $B(x_m, 5h_e)$. Since $\|x_m - p\| - 2\delta > 4h_e$, the absolute value of the integral in equation 3.9 reaches maximum when $\|x + tu - p\|$ reaches its minimum $\|x_m - p\| - 2\delta$ and $|\pi_p(x + tu, n(x))|$ reaches its maximum $\|x_m - p\| + 2\delta$. Hence

$$\begin{aligned}
&|\mathcal{G}_p(x_m, n(x)) - \mathcal{G}_p(x, n(x))| \le e^{-\frac{(\|x_m - p\| - 2\delta)^2}{h_e^2}} \\
&\big(1 - 5\frac{(\|x_m - p\| + 2\delta)^2}{h_e^2} + 2\frac{(\|x_m - p\| + 2\delta)^4}{h_e^4}\big)\|x_m - x\|
\end{aligned}$$

which is a decreasing function of $\|x_m - p\|$ when $\|x_m - p\| > 5h_e$. Decompose the space outside $B(x_m, 5h_e)$ using $(\mathbb{S}_{x_m}(w_i, 5h_e))_{i=1}^{\infty}$ with $w_i = 5ih_e$. If $p \in \mathbb{S}_{x_m}(w_i, 5h_e)$, then

$$\begin{aligned}
&|\mathcal{G}_p(x_m, n(x)) - \mathcal{G}_p(x, n(x))| \\
&\le e^{-\frac{(w_i - 2\delta)^2}{h_e^2}} \big(1 - 5\frac{(w_i + 2\delta)^2}{h_e^2} + 2\frac{(w_i + 2\delta)^4}{h_e^4}\big)\|x_m - x\|
\end{aligned}$$

>From Lemma 2, the number of the sample points is bounded in each $\mathbb{S}_{x_m}(w_i, 5h_e)$. Hence we have

$$\begin{aligned}
&|\sum_{p \notin B(x_m, 5h_e)} (\mathcal{G}_p(x_m, n(x)) - \mathcal{G}_p(x, n(x)))| \\
&\le \frac{C_1}{2\varepsilon^2} \sum_{i=1}^{\infty} (w_i^2 + 5w_i h_e + 25h_e^2) e^{-\frac{(w_i - 2\delta)^2}{h_e^2}} \\
&\left(1 - 5\frac{(w_i + 2\delta)^2}{h_e^2} + 2\frac{(w_i + 2\delta)^4}{h_e^4}\right)\|x_m - x\| \\
&\le \frac{C_1}{\varepsilon^2}(w_1^2 + 5w_1 h_e + 25h_e^2) e^{-\frac{(w_1 - 2\delta)^2}{h_e^2}} \\
&\left(1 - 5\frac{(w_1 + 2\delta)^2}{h_e^2} + 2\frac{(w_1 + 2\delta)^4}{h_e^4}\right)\|x_m - x\| \\
&\le 75C_1 \frac{h_e^2}{\varepsilon^2} e^{-\frac{(5h_e - 2\delta)^2}{h_e^2}} \big(1 - 5\frac{(5h_e + 2\delta)^2}{h_e^2} \\
&+ 2\frac{(5h_e + 2\delta)^4}{h_e^4}\big)\|x_m - x\|
\end{aligned} \tag{3.12}$$

which is less than $0.07\|x_m - x\|$.
Similarly, the absolute value of the integral in equation 3.10 reaches maximum when $|\pi_p(x_m, v(\theta))| = \|x_m - p\|$ since $|\pi_p(x_m, v(\theta))| \le \|x_m - p\|$ and $\|x_m - p\| \ge 5h_e$. We have

$$\begin{aligned}
&|\mathcal{G}_p(x_m, n(x_m)) - \mathcal{G}_p(x_m, n(x))| \le e^{-\frac{\|x_m - p\|^2}{h_e^2}} \\
&\big(3\frac{(\|x_m - p\|)^2}{h_e^2} - 1\big)\|x_m - p\| \angle n(x), n(x_m)
\end{aligned}$$

which is also a decreasing function of $\|x_m - p\|$ when $\|x_m - p\| > 5h_e$. Hence

$$\begin{aligned}
&|\sum_{p \notin B(x_m, 5h_e)} (\mathcal{G}_p(x_m, n(x_m)) - \mathcal{G}_p(x_m, n(x)))| \\
&\le \frac{C_1}{2\varepsilon^2} \sum_{i=1}^{\infty} (w_i^2 + 5w_i h_e + 25h_e^2) e^{-\frac{w_i^2}{h_e^2}} \big(3\frac{w_i^3}{h_e^2} - w_i\big) \angle n(x), n(x_m) \\
&\le 27750 C_1 e^{-25} \frac{h_e^3}{\varepsilon^2} \frac{75\|x_m - x\|}{\sqrt{h_n}}
\end{aligned} \tag{3.13}$$

which is less than $3.0 \times 10^{-4}\|x_m - x\|$.
Second consider a sample point p inside $B(x_m, 5h_e)$. We have

$$\begin{aligned}
&|\pi_p(x + tu, n(x))| \le |\pi_p(x_m, n(x))| + \|x_m - x\| \\
&\le |\pi_p(x_m)| + \|x_m - p\| \angle n(x_m), n(x) + \|x_m - x\|
\end{aligned} \tag{3.14}$$

which is less than $0.25h_e$. Let $t = t_0$ maximizes $\|x + tu - p\|$. Equation 3.9 gives

$$|\mathcal{G}_p(x_m, n(x)) - \mathcal{G}_p(x, n(x))| > 0.5 \times e^{-\frac{\|x + t_0 u - p\|^2}{h_e^2}} \|x_m - x\|. \tag{3.15}$$

Furthermore, $\mathcal{G}_p(x_m, n(x)) - \mathcal{G}_p(x, n(x))$ has the same sign for all the sample points inside $B(x_m, 5h_e)$.
Equation 3.10, 3.11 and the fact $|\pi_p(x_m, v(\theta))| \le |\pi_p(x_m)| +$

$\|x_m - p\| \angle n(x_m), n(x) < 0.15 h_e$ give

$$|\mathcal{G}_p(x_m, n(x_m)) - \mathcal{G}_p(x_m, n(x))| < e^{-\frac{\|x_m - p\|^2}{h_e^2}} \|x_m - p\| \frac{75\|x_m - x\|}{\sqrt{h_n}}. \quad (3.16)$$

Hence,

$$\frac{|\mathcal{G}_p(x_m, n(x_m)) - \mathcal{G}_p(x_m, n(x))|}{|\mathcal{G}_p(x, n(x)) - \mathcal{G}_p(x_m, n(x))|} < 150 \frac{e^{-\frac{\|x_m - p\|^2}{h_e^2}}}{e^{-\frac{\|x + t_0 u - p\|^2}{h_e^2}}} \frac{x_m - p}{\sqrt{h_n}}.$$

Also, since the points $x + t_0 u$ and x_m are on $\ell_{x,n(x)}$ we have

$$\|x + t_0 u - p\|^2 - \|x_m - p\|^2 \leq \pi_p^2(x + t_0 u, n(x))$$

which is less than $0.0625 h_e^2$ from inequality 3.14. Hence

$$|\mathcal{G}_p(x_m, n(x_m)) - \mathcal{G}_p(x_m, n(x))| < \frac{1}{2} |\mathcal{G}_p(x, n(x)) - \mathcal{G}_p(x_m, n(x))| \quad (3.17)$$

In particular, there exists a sample point p_0 inside $B(\tilde{x}_m, \varepsilon)$ based on the sampling condition (i) We have $\|x_m - p_0\| < \varepsilon + \delta$ and $\|x + t_0 u - p_0\| < \varepsilon + 3\delta$. Hence 3.15 and 3.16 give

$$|\mathcal{G}_{p_0}(x_m, n(x)) - \mathcal{G}_{p_0}(x, n(x))| > 0.27 \|x_m - x\| \quad (3.18)$$

$$|\mathcal{G}_{p_0}(x_m, n(x_m)) - \mathcal{G}_{p_0}(x_m, n(x))| < 0.017 \|x_m - x\|. \quad (3.19)$$

By triangle inequality, inequalities 3.12 and 3.18 give

$$|\sum_{p \in p_0 \cup (B(x_m, 5h_e))^c} (\mathcal{G}_p(x_m, n(x)) - \mathcal{G}_p(x, n(x)))| > 0.2 \|x_m - x\|.$$

In addition $\sum_{p \in p_0 \cup (B(x_m, 5h_e))^c} (\mathcal{G}_p(x_m, n(x)) - \mathcal{G}_p(x, n(x)))$ has the same sign as $\mathcal{G}_{p_0}(x_m, n(x)) - \mathcal{G}_{p_0}(x, n(x))$. Similarly from inequalities 3.13 and 3.19 we have

$$|\sum_{p \in p_0 \cup (B(x_m, 5h_e))^c} (\mathcal{G}_p(x_m, n(x_m)) - \mathcal{G}_p(x_m, n(x)))| < 0.02 \|x_m - x\|.$$

Hence,

$$|\sum_{p \in p_0 \cup (B(x_m, 5h_e))^c} (\mathcal{G}_p(x_m, n(x_m)) - \mathcal{G}_p(x_m, n(x)))| < \frac{1}{10} |\sum_{p \in p_0 \cup (B(x_m, 5h_e))^c} (\mathcal{G}_p(x_m, n(x)) - \mathcal{G}_p(x, n(x)))|. \quad (3.20)$$

The theorem follows from the inequalities 3.17, 3.20 and the fact that $\mathcal{G}_p(x_m, n(x)) - \mathcal{G}_p(x, n(x))$ has the same sign for all sample points inside $B(x_m, 5h_e)$. □

4. Isotopy

We have seen that the projection procedure takes any point within $\delta\Sigma$ to a point on the extremal surface in $\delta\Sigma$. Let $W = g^{-1}(0) \bigcap \delta\Sigma$, the subset of $g^{-1}(0)$ inside $\delta\Sigma$. Lemma 13 shows that $\bigtriangledown g$ cannot vanish in $\delta\Sigma$ and hence 0 is a regular value. So, by implicit function theorem W is a compact, smooth surface. Recall that $\nu \colon \mathbb{R}^3 \to \Sigma$ takes a point to its closest point on Σ. Let $\nu|_W$ be the restriction of ν to W. We prove that $\nu|_W$ is a homeomorphism. Since W is included in a topological thickening $\delta\Sigma$ of Σ and W separates the sides of $\delta\Sigma$, we also have W and Σ isotopic in $\mathbb{R}^3$ due to a result of Chazal and Cohen-Steiner [CCS04]. This means that there is a continuous map $F \colon \mathbb{R}^3 \times [0,1] \to \mathbb{R}^3$ so that $F(\cdot, 0)$ is the identity of $\mathbb{R}^3$, $F(W, 1) = \Sigma$ and for each $t \in [0,1]$ $F(\cdot, t)$ is a homeomorphism. So, to prove isotopy we only need to prove that W and Σ are homeomorphic.

Theorem 2 $\nu|_W$ is a homeomorphism.

Proof The function $\nu|_W$ is continuous since ν is. Since W is compact, it is sufficient to show that $\nu|_W$ is surjective and injective which are the statements of Lemma 12 and Lemma 14 respectively. □

4.1. Function g and its gradient

The implicit function $g(x)$ can be written as

$$g(x) = \sum_{p \in P} g_p(x)$$

where

$$g_p(x) = e^{-\frac{\|x - p\|^2}{h_e^2}} \pi_p(x) \big(1 - \frac{\pi_p^2(x)}{h_e^2}\big). \quad (4.21)$$

The gradient of the implicit function $g(x)$

$$\bigtriangledown g(x) = \sum_{p \in P} \bigtriangledown g_p(x)$$

where

$$\bigtriangledown g_p(x) = e^{-\frac{\|x - p\|^2}{h_e^2}} \big[(1 - \frac{3\pi_p^2(x)}{h_e^2}) n(x) + 2(\frac{\pi_p^3(x)}{h_e^4} - \frac{\pi_p(x)}{h_e^2})(x - p) + (1 - \frac{3\pi_p^2(x)}{h_e^2}) J(n(x))(x - p)\big]. \quad (4.22)$$

Here we drop a factor of 2 since it does not affect the sign of $g(x)$ and the direction of $\bigtriangledown g(x)$.

Similar to the function $\mathcal{G}$ in the convergence proof, we decompose the function g into two parts. The sample points outside $B(x, 5h_e)$ have much smaller contribution to g and its gradient $\bigtriangledown g$ at x than that of the sample points inside $B(x, 5h_e)$. Let

$$g(x) = \sum_{p \in B(x, 5h_e)} g_p(x) + \sum_{p \notin B(x, 5h_e)} g_p(x)$$

$$\bigtriangledown g(x) = \sum_{p \in B(x, 5h_e)} \bigtriangledown g_p(x) + \sum_{p \notin B(x, 5h_e)} \bigtriangledown g_p(x).$$

4.2. Surjectivity of $\nu|_W$

To prove that $\nu|_W$ is surjective we use the following lemma which helps us to argue that a normal line $\ell_{z,\tilde{n}_z}$ for any $z \in \Sigma$ always intersects W.

Lemma 11

$$\begin{aligned} g(x) &> 0 \quad \text{if } x \in (2\delta\Sigma - \delta\Sigma) \cap \Omega_O \\ &< 0 \quad \text{if } x \in (2\delta\Sigma - \delta\Sigma) \cap \Omega_I \end{aligned}$$

Proof We prove the first half of the lemma, the second half can be proved similarly. Let $x \in (2\delta\Sigma - \delta\Sigma) \cap \Omega_O$. First consider any sample point p outside $B(x, 5h_e)$. Equation 4.21 gives

$$|g_p(x)| = e^{-\frac{\|x-p\|^2}{h_e^2}} \left|\pi_p(x)\left(1 - \frac{\pi_p^2(x)}{h_e^2}\right)\right|.$$

Since $|\pi_p(x)| \leq \|x-p\|$ and $\|x-p\| \geq 5h_e$, one can verify from the graph of the function $\left|\pi_p(x)\left(1-\frac{\pi_p^2(x)}{h_e^2}\right)\right|$ in terms of $\pi_p(x)$ that it reaches the maximum when $|\pi_p(x)| = \|x-p\|$. It follows that

$$|g_p(x)| \leq e^{-\frac{\|x-p\|^2}{h_e^2}} \left(\frac{\|x-p\|^3}{h_e^2} - \|x-p\|\right)$$

which is a decreasing function of $\|x-p\|$ when $\|x-p\| \geq 5h_e$. We decompose the entire space outside $B(x, 5h_e)$ as we did in the convergence proof. If $p \in \mathbb{S}_x(w_i, 5h_e)$, then

$$|g_p(x)| \leq e^{-\frac{w_i^2}{h_e^2}} \left(\frac{w_i^3}{h_e^2} - w_i\right).$$

Due to Lemma 2, we have an upper bound on the number of the sample points in each $\mathbb{S}_x(w_i, 5h_e)$. Hence we obtain

$$\begin{aligned} \Big|\sum_{p \notin B(x,5h_e)} g_p(x)\Big| &\leq \sum_{p \notin B(x,5h_e)} |g_p(x)| \\ &< \frac{C_1}{2\varepsilon^2} \sum_{i=1}^{\infty} (w_i^2 + 5w_i h_e + 25h_e^2) e^{-\frac{w_i^2}{h_e^2}} \left(\frac{w_i^3}{h_e^2} - w_i\right) \\ &< \frac{C_1}{\varepsilon^2} (w_1^2 + 5w_1 h_e + 25h_e^2) e^{-\frac{w_1^2}{h_e^2}} \left(\frac{w_1^3}{h_e^2} - w_1\right) \\ &< 9000 C_1 e^{-25} \frac{h_e^3}{\varepsilon^2} \end{aligned}$$

which is less than $2.6 \times 10^{-3} h_e$.
Now consider a sample point $p \in B(x, 5h_e)$. We have $0 < \pi_p(x) < 0.135h_e$ and hence $g_p(x) > 0$ from equation 4.21. In particular, there exists a sample point $p_0 \in B(\tilde{x}, \varepsilon)$ by the sampling condition (i). Since $\|x-p\| \leq \varepsilon + 2\delta$ and $\pi_{p_0}(x) > 0.045h_e$ we have

$$g_{p_0}(x) > e^{-\frac{(\varepsilon+2\delta)^2}{h_e^2}} \pi_{p_0}(x)\left(1 - \frac{\pi_{p_0}^2(x)}{h_e^2}\right)$$

which is greater than $0.025h_e$.

Therefore, for any point $x \in (2\delta\Sigma - \delta\Sigma) \cap \Omega_O$

$$\begin{aligned} g(x) &> \sum_{p \in B(x,5h_e)} g_p(x) - \Big|\sum_{p \notin B(x,5h_e)} g_p(x)\Big| \\ &> g_{p_0}(x) - \Big|\sum_{p \notin B(x,5h_e)} g_p(x)\Big| > 0. \end{aligned}$$

□

Lemma 12 $\nu|_W$ is surjective.

Proof Let z be any point in Σ. The normal line $\ell_{z,\tilde{n}(z)}$ intersects $g^{-1}(0)$ within $\delta\Sigma$, thanks to Lemma 11. By definition of W, it intersects W. This means $\nu|_W$ maps a point of W to z or another point $y \in \Sigma \cap \ell_{z,\tilde{n}_z}$. We argue that $y \neq z$ does not exist. For if it does, the distance $\|y-z\|$ has to be more than the distance of z to the medial axis, which is at least 1. However, since both z and y are in $\delta\Sigma$, $\|y-z\| \leq 2\delta < 1$. Therefore, for each point $z \in \Sigma$, there is a point in W which is mapped by $\nu|_W$ to z. □

4.3. Injectivity of $\nu|_W$

The following lemma states that the gradient of g and the normals to the surface Σ cannot be too far apart (proof appears in the appendix). This, in turn, helps us to prove that $\nu|_W$ is injective.

Lemma 13 Let z be any point on Σ, then for any $x \in \ell_{z,\tilde{n}_z} \cap \delta\Sigma$ $\angle \bigtriangledown g(x), \tilde{n}_z < \frac{\pi}{2}$ and $\| \bigtriangledown g(x)\| > 0$.

Lemma 14 $\nu|_W$ is injective.

Proof To prove the injectivity of $\nu|_W$, assume for contradiction that there are two points w and w' in W so that $\nu|_W(w) = \nu|_W(w') = z$. This means $\ell_{z,\tilde{n}_z}$ intersects W at w and w' within $\delta\Sigma$. Without loss of generality assume that w and w' are two such consecutive intersection points. Then, $\ell_{z,\tilde{n}_z}$ makes at least $\frac{\pi}{2}$ angle with one of the normals to W at w and w'. But, that is impossible since by Lemma 13

$$\angle \tilde{n}_z, \bigtriangledown g(x) < \frac{\pi}{2}$$

for any point $x \in \ell_{z,\tilde{n}_z} \delta\Sigma$. □

5. Normal estimation

The computation of the normal vector field n requires assigned normals at the points of P. These assigned normals should approximate the normals at the closest points of Σ. Estimating normals of a surface from a noisy sample is an intriguing problem. We adopt an approach of Dey and Goswami [DG04] to estimate the normals from the Delaunay balls. When the sample points are "noise-free", Amenta and Bern [AB99] showed that the poles (furthest Voronoi vertices) help in estimating the normals. In presence of noise, the centers of relatively big Delaunay balls play the roles of the poles. We show that the vectors from the sample

points incident to such big Delaunay balls towards their centers indeed approximate the normals of Σ. Figure 4 shows an implementation of this concept.

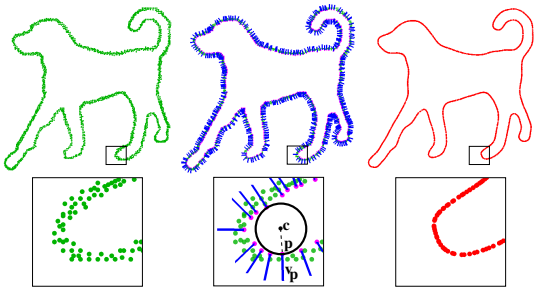

Figure 4: *Outward normals are estimated from big Delaunay balls at a subset of sample points (middle); points after projection with these normals (right).*

Lemma 15 below tells us that normals can be estimated from large Delaunay balls. We prove it in the appendix assuming uniform sampling for P.

Lemma 15 Let $p \in P$ be incident to a Delaunay ball $B(c,r)$ where $r > 1/5$ and $c \in \Omega_O$. Then, $\angle \vec{pc}, \tilde{n}_{\tilde{p}} = O(\varepsilon)$ for a sufficiently small $\varepsilon > 0$.

The next lemma is a direct consequence of Lemma 5 in [DG04] which says that there are many big Delaunay balls.

Lemma 16 For each point $x \in \Sigma$, there is a Delaunay ball containing a medial axis point inside and a sample point on the boundary within $O(\varepsilon)$ distance from x.

Lemma 16 and Lemma 15 together suggest an algorithm for estimating the normals of Σ from P. The big Delaunay balls whose radii are of the order of minimum feature size need to be determined. We compute them by comparing their radii with the nearest neighbor distances of the incident sample points. For a point $p \in P$, let λ_p denote the average nearest distances to the five nearest neighbors of p in P. We determine all Delaunay balls incident to p whose radii are larger than $c\lambda_p$ where k is an user defined parameter. We take $c = 2.5$ in our experiments. Notice that some points in P may not satisfy this condition which means they do not contribute any big Delaunay balls.

The vector from a sample point p to the center of an incident big Delaunay ball estimates the normal at $\tilde{p}$, but without any consistent orientation. In order to orient the normals we determine the big Delaunay balls whose centers lie in the bounded component of $\mathbb{R}^3 \setminus \Sigma$. We follow the algorithm of Dey and Goswami [DG04] to do so. We call them inner big Delaunay balls. The estimated normal at p is the negated average of all directions from p to the centers of all big inner Delaunay balls, see Figure 4.

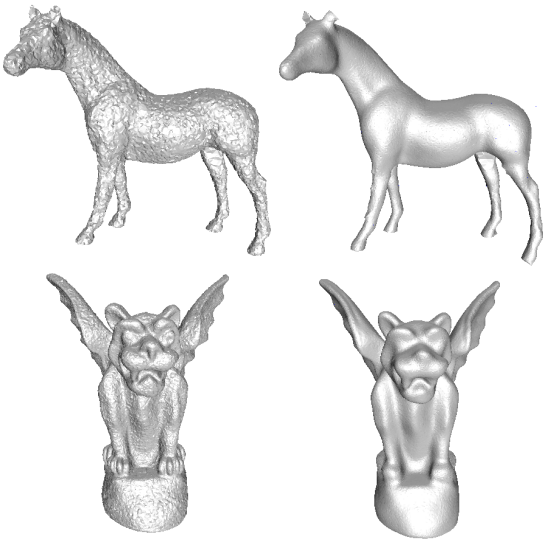

Figure 5: *Reconstruction with Robust Cocone [10] produces unnecessary undulations (left). Reconstruction after smoothing with the projections (right).*

6. Results

We implemented the projection method after estimating the normals with the Delaunay balls. A surface is computed from the projected points with the Tight Cocone algorithm for surface reconstruction [DG03]. Two examples are shown in Figure 5. Figure 6 shows the effect of different values of h_e and h_n on smoothing. As expected, the larger the value of h_e and h_n, the smoother the surface becomes. For computing the normal field and also for the projection, not all sample points are taken as the actual theory dictates. Instead, only a set of nearby points are taken to save the cost of computations. Figure 7 shows a comparison between k-nearest neighbor approach [ABCO*01, ZPKG02] and the points in balls of radius $6 \times max\{h_n, h_e\}$ for these computations.

References

[AA03] ADAMSON A., ALEXA M.: Ray tracing point set surfaces. In *Proc. Shape Modeling Internat.* (2003), pp. 272–279. 1

[AB99] AMENTA N., BERN M.: Surface reconstruction by voronoi filtering. *Discr. Comput. Geom. 22* (1999), 481–504. 3, 8

[ABCO*01] ALEXA M., BEHR J., COHEN-OR D., FLEISHMAN S., LEVIN D., SILVA C.: Point set surfaces. In *Proc. IEEE Visualization* (2001), pp. 21–28. 1, 9

[ACDL02] AMENTA N., CHOI S., DEY T. K., LEEKHA N.: A simple algorithm for homeomorphic surface reconstruction. *Internat. J. Comput. Geom. & Applications 12* (2002), 125–141. 3

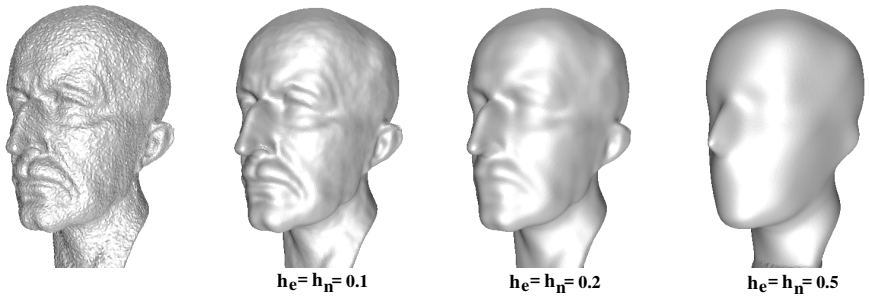

Figure 6: *Smoothing with different values of h_e and h_n.*

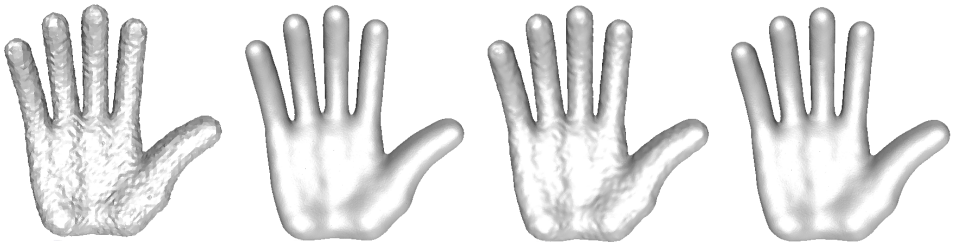

Figure 7: *Second hand is the actual extremal surface while the third one is computed by considering k-nearest neighbors (k=30) and the fourth one is computed by considering samples within a ball whose radius is 6 times of max{h_e, h_n}.*

[AK04] AMENTA N., KIL Y. J.: Defining point-set surfaces. In *Proceedings of ACM SIGGRAPH 2004* (Aug. 2004), ACM Press, pp. 264–270. 1, 2

[BC00] BOISSONNAT J. D., CAZALS F.: Smooth surface reconstruction via natural neighbor interpolation of distance functions. In *Proc. 16th. Annu. Sympos. Comput. Geom.* (2000), pp. 223–232. 3

[CCS04] CHAZAL F., COHEN-STEINER D.: A condition for isotopic approximation. In *Proc. Ninth ACM Sympos. Solid Modeling Appl.* (2004). 7

[DG03] DEY T. K., GOSWAMI S.: Tight cocone: A watertight surface reconstructor. *J. Computing Informat. Sci. Engin. 13* (2003), 302–307. 9

[DG04] DEY T. K., GOSWAMI S.: Provable surface reconstruction from noisy samples. In *Proc. 20th Annu. Sympos. Comput. Geom.* (2004), pp. 330 – 339. 1, 2, 8, 9

[GM97] GUY G., MEDIONI G.: Inference of surfaces, 3d curves and junctions from sparse, noisy, 3d data. *IEEE Trans. Pattern Analysis Machine Intelligence 19* (1997), 1265–1277. 3

[JCCCM*01] J. C. CARR R. K. B., CHERRIE J. B., MITCHELL T. J., FRIGHT W. R., MCCALLUM B. C., EVANS T. R.: Reconstruction and representation of 3d objects with radial basis functions. In *Proceedings of ACM SIGGRAPH 2001* (2001), ACM Press, pp. 67–76. 1

[Kol05] KOLLURI R. D.: provably good moving least squares. *soda 2005* (2005). 1, 3

[KSO04] KOLLURI R. K., SHEWCHUK J. R., O'BRIEN J. F.: Watertight spectral surface reconstruction. In *Proc. Symposium of Geometry Process* (2004). 1

[Lev98] LEVIN D.: The approximation power of moving least-squares. *Math. Computation 67* (1998), 1517–1531. 1, 2

[MVF03] MEDEROS B., VELHO L., FIGUEIREDO L. H. D.: Moving least squares multiresolution surface approximation. In *Proceedings of ACM SIGGRAPH 2003* (2003), ACM Press. 1

[OBA*03] OHTAKE Y., BELYAEV A., ALEXA M., TURK G., SEIDEL H.-P.: Multi-level partition of unity implicits. In *Proceedings of ACM SIGGRAPH 2003* (Aug. 2003), ACM Press, pp. 463–470. 1

[PKKG03] PAULY M., KEISER R., KOBBELT L., GROSS M.: Shape modeling with point-sampled geometry. In *Proceedings of ACM SIGGRAPH 2003* (2003), ACM Press, pp. 641–650. 1

[ZPKG02] ZWICKER M., PAULY M., KNOLL O., GROSS M.: Pointshop 3d: An interactive system for point-based surface editing. In *Proceedings of ACM SIGGRAPH 2002* (2002), ACM Press, pp. 322–329. 1, 9

7. Appendix

Proof of Lemma 8.

Proof Equation 3.7 gives

$$n(x)^T \bigtriangledown_y \mathcal{G}_p(y,n(x)) = e^{-\frac{\|y-p\|^2}{h_e^2}}\big(1-5\frac{\pi_p^2(y,n(x))}{h_e^2} + 2\frac{\pi_p^4(y,n(x))}{h_e^4}\big). \tag{7.23}$$

Consider a sample point p outside $B(x,5h_e)$. Since $\|y-p\| \geq \|x-p\| - 4\delta$ we have

$$n(x)^T \bigtriangledown_y \mathcal{G}_p(y,n(x)) \geq -\frac{17}{8}e^{-\frac{(\|x-p\|-4\delta)^2}{h_e^2}}$$

which is an increasing function of $\|x-p\|$ when $\|x-p\| > 5h_e$. Decompose the space outside $B(x,5h_e)$ using $(\mathbb{S}_x(w_i,5h_e))_{i=1}^{\infty}$ with $w_i = 5ih_e$. If $p \in \mathbb{S}_x(w_i,5h_e)$, then

$$n(x)^T \bigtriangledown_y \mathcal{G}_p(y,n(x)) \geq -\frac{17}{8}e^{-\frac{(w_i-4\delta)^2}{h_e^2}}.$$

Using Lemma 2, which bounds the number of the sample points inside $\mathbb{S}_x(w_i,5h_e)$, we obtain a lower bound on the contribution of the sample points outside $B(x,5h_e)$ to $\mathcal{G}(y,n(x))$.

$$\begin{aligned}
&\sum_{p\notin B(x,5h_e)} \mathcal{G}_p(y,n(x)) \\
&\geq \frac{C_1}{2\varepsilon^2}\sum_{i=1}^{\infty}(w_i^2+5w_ih_e+25h_e^2)\big(-\frac{17}{8}e^{-\frac{(w_i-4\delta)^2}{h_e^2}}\big) \\
&\geq \frac{C_1}{\varepsilon^2}(w_1^2+5w_1h_e+25h_e^2)\big(-\frac{17}{8}e^{-\frac{(w_1-4\delta)^2}{h_e^2}}\big) \\
&\geq -\frac{1275C_1}{8}\frac{h_e^2}{\varepsilon^2}e^{-\frac{(5h_e-4\delta)^2}{h_e^2}}
\end{aligned}$$

which is greater than -3.18×10^{-4}.
Consider a sample point p inside $B(x,5h_e)$. We have $|\pi_p(y,n(x))| \leq |\pi_p(x)| + \|y-x\| < 0.3h_e$. One can verify that $n(x)^T \bigtriangledown_y \mathcal{G}_p(y,n(x)) > 0$ (equation 7.23). In particular, there exists a sample point p_0 inside $B(\tilde{x},\varepsilon)$ so that $\|y-p_0\| \leq \varepsilon+4\delta$. Hence

$$n(x)^T \bigtriangledown_y \mathcal{G}_{p_0}(y,n(x)) \geq 0.5e^{-\frac{(\varepsilon+4\delta)^2}{h_e^2}}$$

which is greater than 0.25. Therefore,

$$\begin{aligned}
&n(x)^T \bigtriangledown_y \mathcal{G}(y,n(x)) = n(x)^T \sum_{p\in B(x,5h_e)} \bigtriangledown_y \mathcal{E}_p(y,n(x)) \\
&+n(x)^T \sum_{p\notin B(x,5h_e)} \bigtriangledown_y \mathcal{E}_p(y,n(x)) > 0.
\end{aligned}$$

□

Proof of Lemma 9.

Proof We show the first half of the lemma and the second half can be proved symmetrically. Consider a sample point p outside $B(x,5h_e)$. Since $\|x_+ - p\| \geq \|x-p\| - 2\delta$ and $\pi_p(x_+,n(x)) \leq \|x-p\| + 2\delta$ equation 3.6 gives

$$\begin{aligned}
|\mathcal{G}_p(x_+,n(x))| \leq& e^{-\frac{(\|x-p\|-2\delta)^2}{h_e^2}}\big(\frac{(\|x-p\|+2\delta)^3}{h_e^2} \\
&-(\|x-p\|+2\delta)\big)
\end{aligned}$$

which is a decreasing function of $\|x-p\|$ when $\|x-p\| > 5h_e$. Hence we have

$$\begin{aligned}
&|\sum_{p\notin B(x,5h_e)} \mathcal{G}_p(x_+,n(x))| \leq \frac{C_1}{2\varepsilon^2}\sum_{i=1}^{\infty}(w_i^2+5w_ih_e+25h_e^2) \\
&e^{-\frac{(w_i-2\delta)^2}{h_e^2}}\big(\frac{(w_i+2\delta)^3}{h_e^2}-(w_i+2\delta)\big) \\
&\leq 75C_1\frac{h_e^2}{\varepsilon^2}e^{-\frac{(5h_e-2\delta)^2}{h_e^2}}\big(\frac{(5h_e+2\delta)^3}{h_e^2}-(5h_e+2\delta)\big)
\end{aligned}$$

which is less than $7.25\times10^{-3}h_e$.
Now consider a sample point p inside $B(x,5h_e)$. One can verify that p is in between the planes $\mathcal{P}_+$ and $\mathcal{P}_-$. So $\pi_p(x_+,n(x)) > 0$ and $|\pi_p(x_+,n(x))| < \|x_+ - x_-\| \leq 2\delta$, see Figure 3. Hence we have $\mathcal{G}_p(x_+,n(x)) > 0$ from equation 3.6. In particular, there exists a sample point p_0 inside $B(\tilde{x},\varepsilon)$. We have $\|x_+ - p_0\| \leq \varepsilon+2\delta$ and $\pi_{p_0}(x_+,n(x)) = \pi_{p_0}(a,n(x)) > 0.045h_e$ from Observation 3. Hence

$$\mathcal{G}_{p_0}(x_+,n(x)) > e^{-\frac{(\varepsilon+2\delta)^2}{h_e^2}}\pi_{p_0}(x_+,n(x))(1-\frac{\pi_{p_0}^2(x_+,n(x)}{h_e^2})$$

which is greater than $2.63\times10^{-2}h_e$. Therefore,

$$\begin{aligned}
&\mathcal{G}(x_+,n(x)) \\
&\geq |\sum_{p\in B(x,5h_e)} \mathcal{G}_p(x_+,n(x))| - |\sum_{p\notin B(x,5h_e)} \mathcal{G}_p(x_+,n(x))| \\
&> \mathcal{G}_{p_0}(x_+,n(x)) - |\sum_{p\notin B(x,5h_e)} \mathcal{G}_p(x_+,n(x))| > 0.
\end{aligned}$$

□

Proof of Observation 1.

Proof The condition $\angle m,\tilde{n}_{\tilde{x}} < \frac{\pi}{2} - asin\frac{(r+\delta)^2+\varepsilon^2}{r+\delta}$ forces that the line $\ell_{\tilde{x},m}$ intersect the planes $\mathcal{P}_-$ and $\mathcal{P}_+$ inside $B(\tilde{x},r+\delta)$. One can verify that $|m^T(p_j-p_i)|$ reaches the maximum when x is on $\Sigma_{+\delta}$, $p_i(p_j)$ is on $\mathcal{P}_-(\mathcal{P}_+)$ and the segment p_ip_j is a diameter of $B(\tilde{x},r+\delta)$. Hence

$$\begin{aligned}
&|m^T(p_j-p_i)| \leq 2|m^T(p_j-\tilde{x})| \\
&\leq 2(r+\delta)cos(\angle\tilde{n}_{\tilde{x}},(p_j-\tilde{x})-\angle m,\tilde{n}_{\tilde{x}}) \\
&\leq 2(r+\delta)(cos\angle\tilde{n}_{\tilde{x}},(p_j-\tilde{x})+sin\angle m,\tilde{n}_{\tilde{x}}) \\
&\leq 2((r+\delta)^2+\varepsilon^2+(r+\delta)\angle m,\tilde{n}_{\tilde{x}}.
\end{aligned}$$

□

Proof of Observation 2.

Proof The condition $\angle m,\tilde{n}_{\tilde{x}} < \frac{\pi}{2} - asin\frac{\delta+(r+\delta)^2+\varepsilon^2}{r+\delta}$ forces that the line $\ell_{x,m}$ intersect the planes $\mathcal{P}_-$ and $\mathcal{P}_+$ inside

$B(\tilde{x}, r+\delta)$. So $|\pi_p(x,m)|$ reaches the maximum if x is on $\Sigma_{+\delta}$ and p is on $\mathcal{P}_-$. Hence

$$|\pi_p(x,m)| \leq (\delta + (r+\delta)^2 + \varepsilon^2) + d(p, \ell_{\tilde{x},\tilde{n}_{\tilde{x}}}) \angle m, \tilde{n}_{\tilde{x}}.$$

□

Proof of Observation 3.

Proof We only prove the first half and the second half can be proved similarly. For $x \in (2\delta\Sigma - \delta\Sigma) \cap \Omega_O$, the condition $\angle m, \tilde{n}_{\tilde{x}} < atan\frac{\delta-(r+\delta)^2-\varepsilon^2}{r+\delta}$ forces that the intersection point between the line through x with normal m and the plane $\mathcal{P}_+$ be outside $B(\tilde{x}, r+\delta)$. As a result, $\pi_p(x,m)$ becomes minimal if x is on $\Sigma_{+\delta}$ and p is on $\mathcal{P}_+$. Hence

$$\pi_p(x,m) \geq (\delta - (r+\delta)^2 - \varepsilon^2) cos\angle m, \tilde{n}_{\tilde{x}} - d(p, \ell_{\tilde{x},\tilde{n}_{\tilde{x}}}) sin\angle m, \tilde{n}_{\tilde{x}} \geq E.$$

□

The proof for the normal lemmas below is based on the observation that the sample points outside $B(x, 6h_n)$ have little effect on $n(x)$ since the weight of the sample point outside $B(x, 6h_n)$ is less than $e^{-36} \approx 2.31 \times 10^{-16}$. To take advantage of this fact we decompose $Aw(x)$ as follows:

$$Aw(x) = A_I w_I(x) + A_O w_O(x)$$

where A_I is the row vector of the equipped normals of the samples inside $B(x, 6h_n)$ and A_O is the row vector of normals of the samples outside $B(x, 6h_n)$. $w_I(x)$ is the column vector of weights of the samples inside $B(x, 6h_n)$ for x and $w_O(x)$ is the column vector of weights of the samples outside $B(x, 6h_n)$ for x. In addition, in the following proofs for the normal lemmas we decompose the space outside $B(x, 6h_n)$ using $(\mathbb{S}_x(w_i, 6h_n)_{i=1}^{\infty}$ with $w_i = 6ih_n$.

Lemma 17 If $\varepsilon < 0.1$ and $h_n \geq 8\varepsilon$, then for any $x \in 2\delta\Sigma$ with $\delta = 0.08\varepsilon$

$$\|w_I(x)\|_1 > 2$$

where $\|v\|_1$ is the 1-norm of the vector v, which is the summation of all the components of v.

Proof There exists a sample point inside $B(\tilde{x}, \varepsilon)$ from the sampling condition (i). In addition, $S(\tilde{x}, 2\varepsilon)$ and $S(\tilde{x}, 4\varepsilon)$ intersect Σ since the local feature size of Σ at any point is greater or equal to 1. Hence, there exists a sample point inside $\mathbb{S}_{\tilde{x}}(\varepsilon, 2\varepsilon)$ and $\mathbb{S}_{\tilde{x}}(3\varepsilon, 2\varepsilon)$ respectively from the sampling conditions. Hence

$$\|w_I(x)\|_1 > e^{-\frac{(\delta+\varepsilon)^2}{h_n^2}} + e^{-\frac{(\delta+3\varepsilon)^2}{h_n^2}} + e^{-\frac{(\delta+5\varepsilon)^2}{h_n^2}} > 2.$$

□

Lemma 18 If $h_n \leq 0.01$, $10\varepsilon \leq h_n \leq 1000\varepsilon$ and $\alpha \leq 10$, then for any point $x \in 2\delta\Sigma$ with $\delta = 0.08\varepsilon$,

$$\|Aw(x)\| \geq \left((1-4C_2^2)^{\frac{1}{4}} - 108C_1\frac{h_n^2}{\varepsilon^2}e^{-36}\right)\|w_I(x)\|_1 \quad (7.24)$$

and

$$\|w(x)\|_1 \leq \left(1 + 108C_1\frac{h_n^2}{\varepsilon^2}e^{-36}\right)\|w_I(x)\|_1. \quad (7.25)$$

Proof
First, we could have an upper bound of the weights for the sample points outside $B(x, 6h_n)$ since the number of the sample points inside each $\mathbb{S}_x(w_i, 6h_n)$ can be bounded due to Lemma 2.

$$\|w_O(x)\|_1 \leq \frac{C_1}{2\varepsilon^2}\sum_{i=1}^{\infty}(w_i^2 + 6w_ih_n + 36h_n^2)e^{-\frac{w_i^2}{h_n^2}} \leq 108C_1\frac{h_n^2}{\varepsilon^2}e^{-36}.$$

We have $\|w_I(x)\|_1 > 2$ from Lemma 17, hence

$$\|w_O(x)\|_1 \leq 108C_1\frac{h_n^2}{\varepsilon^2}e^{-36}\|w_I(x)\|_1. \quad (7.26)$$

Second, we find the lower bound for $\|A_I w_I(x)\|$.

$$\|A_I w_I(x)\| = \sqrt{|(A_I w_I(x))^T (A_I w_I(x))|} = \sqrt{|\sum_{p_i,p_j \in B(x,6h_n)} w_{p_i}(x) w_{p_j}(x) v_{p_i}^T v_{p_j}|}.$$

>From Lemma 3, $v_{p_i}^T v_{p_j} = cos\angle v_{p_i}, v_{p_j} \geq \sqrt{1-4C_2^2}$ which gives

$$\|A_I w_I(x)\| \geq (1-4C_2^2)^{\frac{1}{4}}\|w_I(x)\|_1.$$

We obtain inequality 7.24 from $\|Aw(x)\| \geq \|A_I w_I(x)\| - \|w_O(x)\|_1$ and inequality 7.25 from $\|w(x)\|_1 = \|w_I(x)\|_1 + \|w_O(x)\|_1$ □

Proof of Lemma 5.

Proof

$$n(x) = \frac{A_I w_I(x)}{\|Aw(x)\|} + \frac{A_O w_O(x)}{\|Aw(x)\|}$$

We have shown $\angle \tilde{n}_{\tilde{x}}, v_p \leq C_2$ for any sample point $p \in B(x, 6h_n)$ in the proof of Lemma 3. Hence $\angle \tilde{n}_{\tilde{x}}, \frac{A_I w_I(x)}{\|Aw(x)\|}$ is also less than or equal to C_2.
Equation 7.26 gives

$$\|A_O w_O(x)\| \leq \|w_O(x)\|_1 \leq 108C_1\frac{h_n^2}{\varepsilon^2}e^{-36}\|w_I(x)\|_1.$$

In addition $C_2 < 0.075$ and $108C_1\frac{h_n^2}{\varepsilon^2}e^{-36} < 4 \times 10^{-4}$ under the given conditions. Hence,

$$|\|A_I w_I(x)\| - \|A_O w_O(x)\|| = \|A_I w_I(x)\| - \|A_0 w_O(x)\| \geq \left((1-4C_2^2)^{\frac{1}{4}} - 108C_1\frac{h_n^2}{\varepsilon^2}e^{-36}\right)\|w_I(x)\|_1.$$

One can verify that

$$\angle n(x), \frac{A_I w_I(x)}{\|Aw(x)\|} \leq asin\frac{\|A_O w_O(x)\|}{\|\|A_I w_I(x)\| - \|A_O w_O(x)\|\|}$$
$$\leq asin\frac{108C_1\frac{h_n^2}{\varepsilon^2}e^{-36}}{(1-4C_2^2)^{\frac{1}{4}} - 108C_1\frac{h_n^2}{\varepsilon^2}e^{-36}}$$

which is less than $216C_1\frac{h_n^2}{\varepsilon^2}e^{-36}$.
The lemma follows from the fact $\angle n(x), \tilde{n}_{\tilde{x}} \leq \angle n(x), \frac{A_I w_I(x)}{\|Aw(x)\|} + \angle \tilde{n}_{\tilde{x}}, \frac{A_I w_I(x)}{\|Aw\|}$. □

Proof of Lemma 6.

Proof We have

$$\|J(n(x))\| \leq \big(1 + \frac{\|(Aw(x))(Aw(x))^T\|}{(Aw(x))^T(Aw(x))}\big)\frac{\|Aw'(x)\|}{\|Aw(x)\|}.$$

It can be shown that $\|(Aw(x))(Aw(x))^T\| = (Aw(x))^T(Aw(x))$. So,

$$\|J(n(x))\| \leq 2\frac{\|Aw'(x)\|}{\|Aw(x)\|}.$$

We have $\|Aw'(x)\| \leq \|A_I w_I'(x)\| + \|A_O w_O'(x)\|$. First we find an upper bound for $\|A_I w_I'(x)\|$.

$$\|A_I w_I'(x)\| \leq \frac{2}{h_n^2}\sum_{p\in B(x,6h_n)} w_p(x)\|v_p(x-p)^T\|.$$

Since v_p is a unit vector, one can prove that $\|v_p(x-p)^T\| = \|x-p\|$, which is less than $6h_n$ for any $p \in B(x,6h_n)$. Therefore,

$$\|A_I w_I'(x)\| \leq \frac{12}{h_n}\|w_I(x)\|_1.$$

Similarly we have

$$\|A_O w_O'(x)\| \leq \frac{2}{h_n^2}\sum_{p\notin B(x,6h_n)} w_p(x)\|x-p\|.$$

Using the decomposition strategy for the proof of the normal lemmas, we have

$$\|A_O w_O'(x)\| \leq \frac{2}{h_n^2}\frac{C_1}{2\varepsilon^2}\sum_{i=1}^{\infty}(w_i^2 + 6w_i h_n + 36h_n^2)e^{-\frac{w_i^2}{h_n^2}}w_i$$
$$\leq \frac{12}{h_n}108C_1\frac{h_n^2}{\varepsilon^2}e^{-36}.$$

Under the given conditions $\|w_I(x)\|_1 > 2$. So, we have

$$\|Aw'(x)\| \leq \frac{12}{h_n}\big(1 + 108C_1\frac{h_n^2}{\varepsilon^2}e^{-36}\big)\|w_I(x)\|_1.$$

Equation 7.24 gives

$$\frac{\|Aw'(x)\|}{\|Aw(x)\|} \leq C_3\frac{12}{h_n}. \tag{7.27}$$

□

Proof of Lemma 7.

Proof Let $u = \frac{y-x}{\|y-x\|}$, which is either $n(x)$ or $-n(x)$ since y is on $\ell_{x,n(x)}$. We can express $n(y)$ as

$$n(y) = n(x) + \int_0^{\|y-x\|} J(n(x+tu))u\,dt \tag{7.28}$$

from which we get

$$n(x)^T n(y) = 1 + \int_0^{\|y-x\|} n(x)^T J(n(x+tu))u\,dt$$
$$\geq 1 - \int_0^{\|y-x\|}\|n(x)\|\|J(n(x+tu))\|dt. \tag{7.29}$$

We need to find an upper bound for

$$\|n(x)\|\|J(n(x+tu))\| \leq \frac{1}{\|Aw(x)\|\|Aw(x+tu)\|^2}$$
$$\|(Aw(x))^T(Aw(x+tu))^T(Aw(x+tu))$$
$$-(Aw(x))^T(Aw(x+tu))(Aw(x+tu))^T\|\frac{\|Aw'(x+tu)\|}{\|Aw(x+tu)\|}. \tag{7.30}$$

Since $x+tu \in \delta\Sigma$, equation 7.27 gives

$$\frac{\|Aw'(x+tu)\|}{\|Aw(x+tu)\|} \leq C_3\frac{12}{h_n}. \tag{7.31}$$

Similar to the bounds for $\|w_I(x)\|_1$, $\|Aw(x)\|$ and $\|w(x)\|_1$, we can have bounds for $\|w_I(x+tu)\|_1$, $\|Aw(x+tu)\|$ and $\|w(x+tu)\|_1$ with $t \leq 2\delta$, i.e.,

$$\|w_I(x+tu)\|_1 > 2 \tag{7.32}$$

and

$$\|Aw(x+tu)\| \geq \big((1-4C_2^2)^{\frac{1}{4}} - 108C_1\frac{h_n^2}{\varepsilon^2}e^{-\frac{(6h_n-2\delta)^2}{h_n^2}}\big)$$
$$\|w_I(x+tu)\|_1 \tag{7.33}$$

and

$$\|w(x+tu)\|_1 \leq \big(1 + 108C_1\frac{h_n^2}{\varepsilon^2}e^{-\frac{(6h_n-2\delta)^2}{h_n^2}}\big)\|w_I(x+tu)\|_1. \tag{7.34}$$

Notice that $\|w_I(x+tu)\|_1$ is the summation of the weights for the sample points inside $B(x,6h_n)$ rather than $B(x+tu,6h_n)$.
Now we compute an upper bound for the following term with $0 \leq t \leq \|y-x\|$.

$$\|(Aw(x))^T(Aw(x+tu))^T(Aw(x+tu))$$
$$-(Aw(x))^T(Aw(x+tu))(Aw(x+tu))^T\|$$
$$= \|\sum_{p_i,p_j,p_k\in P}\big[w_{p_i}(x)w_{p_j}(x+tu)w_{p_k}(x+tu)$$
$$-w_{p_i}(x+tu)w_{p_j}(x)w_{p_k}(x+tu)\big](v_{p_j}^T v_{p_k})v_{p_i}^T\|$$
$$\leq \|w(x+tu)\|_1\sum_{p_i,p_j\in P} w_{p_i}(x)w_{p_j}(x+tu)\big|1 - e^{-2\frac{u^T(p_j-p_i)t}{h_n^2}}\big|.$$

Partition $\sum_{p_i,p_j\in P} w_{p_i}(x)w_{p_j}(x+tu)\left|1-e^{-2\frac{u^T(p_j-p_i)t}{h_n^2}}\right|$ into four parts depending on whether p_i or p_j is inside $B(x,6h_n)$ or not.

In case both p_i and p_j are inside $B(x,6h_n)$, we have $\angle n(x),\tilde{n}_{\tilde{x}} < 8.12h_n$ from Lemma 5 under the given condition. Hence $|u^T(p_j-p_i)| < 170h_n^2$ from Observation 1. Therefore,

$$\sum_{p_i,p_j\in B(x,6h_n)} w_{p_i}(x)w_{p_j}(x+tu)\left|1-e^{-2\frac{u^T(p_j-p_i)t}{h_n^2}}\right| \leq \|w(x)\|_1\|w(x+tu)\|_1(e^{340t}-1)$$

which is less than $375t\|w(x)\|_1\|w(x+tu)\|_1$ since $t\leq 2\delta\leq 1.6\times10^{-4}$ and $e^{340t}-1<375t$.

In case p_i is inside $B(x,6h_n)$ while p_j is not, we have $|u^T(p_j-p_i)|\leq w_i+12h_n$ if $p_j\in\mathbb{S}_x(w_i,6h_n)$. So,

$$\begin{aligned}&\sum_{\substack{p_i\in B(x,6h_n)\\ p_j\notin B(x,6h_n)}} w_{p_i}(x)w_{p_j}(x+tu)\left|1-e^{-2\frac{u^T(p_j-p_i)t}{h_n^2}}\right|\\ &\leq \frac{C_1}{2\varepsilon^2}\sum_{i=1}^{\infty}(w_i^2+6w_ih_n+36h_n^2)e^{-\frac{(w_i-2\delta)^2}{h_n^2}}\left(e^{2\frac{w_i+12h_n}{h_n^2}t}-1\right)\\ &\leq 108C_1\frac{h_n^2}{\varepsilon^2}e^{-\frac{(6h_n-2\delta)^2}{h_n^2}}\left(e^{\frac{36t}{h_n}}-1\right)\end{aligned}$$

which is less than t since $\frac{t}{h_n}<0.016$ and hence $e^{\frac{36t}{h_n}}-1<60\frac{t}{h_n}$. Similarly, the same upper bound holds when p_j is inside $B(x,6h_n)$ and p_i is not.

When both p_i and p_j are not inside $B(x,6h_n)$, we have $|u^T(p_j-p_i)|\leq w_i+w_j+12h_n$ if $p_i\in\mathbb{S}_x(w_i,6h_n)$ and $p_j\in\mathbb{S}_x(w_j,6h_n)$. Hence,

$$\begin{aligned}&\sum_{\substack{p_i\notin B(x,6h_n)\\ p_j\notin B(x,6h_n)}} w_{p_i}(x)w_{p_j}(x+tu)\left|1-e^{-2\frac{u^T(p_j-p_i)t}{h_n^2}}\right|\\ &\leq \frac{C_1^2}{4\varepsilon^4}\sum_{\substack{1\leq i\leq\infty\\ 1\leq j\leq\infty}}(w_i^2+6w_ih_n+36h_n^2)(w_j^2+6w_jh_n+36h_n^2)\\ &e^{-\frac{w_i^2}{h_n^2}}e^{-\frac{(w_j-2\delta)^2}{h_n^2}}\left(e^{2\frac{w_i+w_j+12h_n}{h_n^2}t}-1\right)\\ &\leq 108^2C_1^2\frac{h_n^4}{\varepsilon^4}e^{-36}e^{-\frac{(6h_n-2\delta)^2}{h_n^2}}\left(e^{\frac{48t}{h_n}}-1\right)\end{aligned}$$

which is less than $10^{-3}t$ since $\frac{t}{h_n}<0.016$ and hence $e^{\frac{48t}{h_n}}-1<75\frac{t}{h_n}$.

Since $\|w(x)\|_1>2$ and $\|w(x+tu)\|_1>2$, we have

$$\begin{aligned}&\|(Aw(x))^T(Aw(x+tu))^T(Aw(x+tu))\\ &-(Aw(x))^T(Aw(x+tu))(Aw(x+tu))^T\|\\ &\leq 400t\|w(x)\|_1\|w(x+tu)\|_1^2.\end{aligned}\tag{7.35}$$

We obtain from inequalities 7.30, 7.31 and 7.35

$$\begin{aligned}\|n(x)\|\|J(n(x+tu))\| &\leq 4800C_3\frac{t}{h_n}\frac{\|w(x)\|_1\|w(x+tu)\|_1^2}{\|Aw(x)\|\|Aw(x+tu)\|^2}\\ &\leq 4800C_3^2C_4^2\frac{t}{h_n}\end{aligned}$$

where

$$C_4=\frac{\left(1+108C_1\frac{h_n^2}{\varepsilon^2}e^{-\frac{(6h_n-2\delta)^2}{h_n^2}}\right)}{\left((1-4C_2^2)^{\frac14}-108C_1\frac{h_n^2}{\varepsilon^2}e^{-\frac{(6h_n-2\delta)^2}{h_n^2}}\right)}.$$

Integrating the integral in 7.29 we obtain

$$n(x)^Tn(y)\geq 1-2400C_3^2C_4^2\frac{\|y-x\|^2}{h_n}.$$

Hence,

$$sin\angle n(x),n(y)\leq\sqrt{4800}C_3C_4\frac{\|y-x\|}{\sqrt{h_n}}$$

where C_3 and C_4 are close to 1 under the given conditions and hence $\angle n(x),n(y)$ is small. One can verify that

$$\angle n(x),n(y)\leq\frac{75\|y-x\|}{\sqrt{h_n}}.$$

□

Proof of Lemma 13.

Proof Since $n(x)$ and $J(n(x))(x-p)$ are perpendicular for any $p\in P$ (Lemma 4), equation 4.22 gives

$$\begin{aligned}\|\nabla g_p(x)\| &\leq e^{-\frac{\|x-p\|^2}{h_e^2}}\left(2\left|\frac{\pi_p^3(x)}{h_e^4}-\frac{\pi_p(x)}{h_e^2}\right|\|x-p\|\right.\\ &\left.+\left|1-\frac{3\pi_p^2(x)}{h_e^2}\right|\sqrt{1+\|J(n(x))\|^2\|(x-p)\|^2}\right).\end{aligned}$$

Consider a sample point p outside $B(x,5h_e)$. Since $|\pi_p(x)|\leq\|x-p\|$ and $\|x-p\|\geq 5h_e$, $|\frac{\pi_p^3(x)}{h_e^4}-\frac{\pi_p(x)}{h_e^2}|$ and $|1-\frac{3\pi_p^2(x)}{h_e^2}|$ reaches maximum when $\pi_p(x)=\|x-p\|$

$$\begin{aligned}\|\nabla g_p(x)\| &\leq e^{-\frac{\|x-p\|^2}{h_e^2}}\left(2\frac{\|x-p\|^4}{h_e^4}-2\frac{\|x-p\|^2}{h_e^2}\right.\\ &\left.+\left(\frac{3\|x-p\|^2}{h_e^2}-1\right)\sqrt{1+\|J(n(x))\|^2\|x-p\|^2}\right)\end{aligned}$$

which is a decreasing function of $\|x-p\|$ when $\|x-p\|>5h_e$. Hence we have

$$\begin{aligned}&\|\sum_{p\notin B(x,5h_e)}\nabla g_p(x)\|\leq\sum_{p\notin B(x,5h_e)}\|\nabla g_p(x)\|\\ &\leq\frac{C_1}{2\varepsilon^2}\sum_{i=1}^{\infty}(w_i^2+5w_ih_e+25h_e^2)e^{-\frac{w_i^2}{h_e^2}}\left(2\frac{w_i^4}{h_e^4}-2\frac{w_i^2}{h_e^2}\right.\\ &\left.+\left(\frac{3w_i^2}{h_e^2}-1\right)\sqrt{1+\|J(n(x))\|^2w_i^2}\right)\\ &\leq 75C_1e^{-25}\frac{h_e^2}{\varepsilon^2}\left(1200+74\sqrt{1+25\|J(n(x))\|^2h_e^2}\right)\end{aligned}\tag{7.36}$$

which is less than 0.03 since we have $\|J(n(x))\|h_e < 0.4$ from Lemma 6.

Now consider a sample point p inside $B(x,5h_e)$ and evaluate the angle between $\bigtriangledown g_p(x)$ and $n(x)$.

$$n(x)^T \bigtriangledown g_p(x) = e^{-\frac{\|x-p\|^2}{h_e^2}}\left(1-5\frac{\pi_p^2(x)}{h_e^2}+2\frac{\pi_p^4(x)}{h_e^4}\right) \quad (7.37)$$

which is greater than $0.96e^{-\frac{\|x-p\|^2}{h_e^2}}$ since $|\pi_p(x)| < 0.085h_e$ for any $x \in \delta\Sigma$. In addition,

$$\|\bigtriangledown g_p(x)\| \le e^{-\frac{\|x-p\|^2}{h_e^2}}\left(10\left|\frac{\pi_p^3(x)}{h_e^4}-\frac{\pi_p(x)}{h_e^2}\right|h_e + \left|1-\frac{3\pi_p^2(x)}{h_e^2}\right|\sqrt{1+25\|J(n(x))\|^2h_e^2}\right)$$

which is less than $3.1e^{-\frac{\|x-p\|^2}{h_e^2}}$. Hence

$$\angle n(x), \bigtriangledown g_p(x) = acos\left(\frac{n(x)^T \bigtriangledown g_p(x)}{\|\bigtriangledown g_p(x)\|}\right) < 1.26. \quad (7.38)$$

In particular, there exists a sample point $p_0 \in B(\tilde{x},\varepsilon)$ from the sampling condition (i) so that $\|x-p_0\| \le \delta+\varepsilon$. We have

$$\|\bigtriangledown g_{p_0}(x)\| \le e^{-\frac{\|x-p_0\|^2}{h_e^2}}\left(2\left|\frac{\pi_{p_0}^3(x)}{h_e^4}-\frac{\pi_{p_0}(x)}{h_e^2}\right|(\delta+\varepsilon) + \left|1-\frac{3\pi_{p_0}^2(x)}{h_e^2}\right|\sqrt{1+\|J(n(x))\|^2(\delta+\varepsilon)^2}\right)$$

which is less than $1.24e^{-\frac{\|x-p\|^2}{h_e^2}}$. So

$$\angle n(x), \bigtriangledown g_{p_0}(x) = acos\left(\frac{n(x)^T \bigtriangledown g_{p_0}(x)}{\|\bigtriangledown g_{p_0}(x)\|}\right) < 0.69.$$

In addition, equation 7.37 gives

$$\|\bigtriangledown g_{p_0}(x)\| \ge n(x)^T \bigtriangledown g_{p_0}(x) > 0.6. \quad (7.39)$$

Inequalities 7.36 and 7.39 give

$$\angle \bigtriangledown g_{p_0}(x), \left(\bigtriangledown g_{p_0}(x) + \sum_{p\notin B(x,5h_e)} \bigtriangledown g_p(x)\right) \le asin\frac{\|\sum_{p\notin B(x,5h_e)} \bigtriangledown g_p(x)\|}{\left|\|\bigtriangledown g_{p_0}(x)\| - \|\sum_{p\notin B(x,5h_e)} \bigtriangledown g_p(x)\|\right|} < 0.06.$$

Hence,

$$\angle n(x), \left(\bigtriangledown g_{p_0}(x) + \sum_{p\notin B(x,5h_e)} \bigtriangledown g_p(x)\right) < 0.75. \quad (7.40)$$

The first part of the lemma follows from inequalities 7.38 and 7.40 and the fact $\angle n(x), \tilde{n}_{\tilde{x}} < 6.5\times10^{-3}$.

>From inequality 7.37, we have $n(x)^T \bigtriangledown g_p(x) > 0$ for all sample point $p \in B(x,5h_e)$. Hence

$$\|\bigtriangledown g(x)\| > n(x)^T \bigtriangledown g_{p_0}(x) - \|\sum_{p\notin B(x,5h_e)} \bigtriangledown g_p(x)\| > 0$$

□

The following lemma is used to prove the guarantee about normal estimation in Lemma 15.

Lemma 19 Let D and D' be two parallel disks within distance of δr in a ball $B = B(c,r)$ having the center c on the same side. Let the angle between D and the boundary of B be more than 2θ. Further, let $q \in D$ be a point where $d(q,\partial D) \ge kr$ and $q' \in \partial B$ be a point where qq' is perpendicular to D. Then, we have (i) $\|q-q'\| > kr\tan\theta$ and (ii) $d(q,\partial D') > kr - \frac{\delta r}{\tan\theta}$.

Proof We assume that D is larger than D' and prove the lemma. The other case where D is smaller than D' can be handled similarly achieving even a better bound. Refer to Figure 7 for all references of labels. Let p be the closest point of q on ∂D. We are given that $\|p-q\| \ge kr$. We have $\|a-t\| > (1-\cos2\theta)r$ and $\|p-a\| < r\sin2\theta$. Consider the similar triangles *pat* and *pqu*. We have

$$\|q-u\| = \frac{\|p-q\|\cdot\|a-t\|}{\|p-a\|} > \frac{kr(1-\cos2\theta)r}{r\sin2\theta} > kr\tan\theta.$$

Since $\|q-q'\| > \|q-u\|$, we have the claim (i). To prove claim (ii), consider the similar triangles *pqu* and *wsu* and use the facts $d(q,\partial D') > \|s-w\|$, $\|q-s\| < \delta r$ and $\|s-u\| > \|q-u\| - \delta r > kr\tan\theta - \delta r$. □

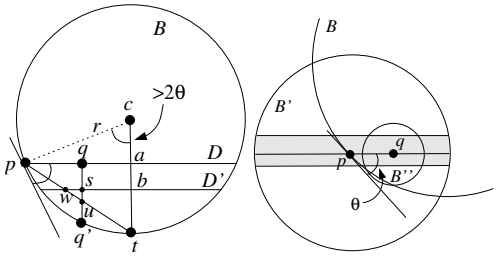

Figure 8: *Illustration for Lemma 19 on the left. Illustration for Lemma 15 on the right.*

Proof of Lemma 15.

Proof Let $B = B(c,r)$. Assume that $\vec{pc}$ makes an angle θ with the normal $\tilde{n}_{\tilde{p}}$. We claim that, if $\theta > 600\varepsilon$, the ball B contains a point of P inside contradicting the fact that B is a Delaunay ball.

Consider the slab L_p with width $2\times101\varepsilon^2$ for the point $\tilde{p}$ delimited by two planes $\mathcal{P}_+$ and $\mathcal{P}_-$ as stated in Lemma 1. The ball $B(\tilde{p},10\varepsilon)$ contains Σ and points from P only within L_p due to Lemma 1. Since $\|p-\tilde{p}\| \le \varepsilon^2$, the ball $B' = B(p,9\varepsilon)$ is contained within $B(\tilde{p},10\varepsilon)$ and thus contains Σ and points from P only within L_p.

Let N_p denote the plane passing through p and with the normal $\tilde{n}_{\tilde{p}}$. Consider the disk D in which B intersects N_p. Let q be a point on the diameter of D passing through p where $\|p-q\| = 4\varepsilon$ for sufficiently small ε. By Lemma 19 $d(q,\partial B) > 4\varepsilon\tan\frac{\theta}{2} > 400\varepsilon^2$.

The distance of q from the bounding planes of L_p is at most $202\varepsilon^2$. This means both of these bounding planes intersect B. Let D' and D'' be the disks in which $\mathcal{P}_+$ and $\mathcal{P}_-$ intersect B. By Lemma 19 the boundaries of D' and D'' are at

least $4\varepsilon - \frac{202\varepsilon^2}{\tan 300\varepsilon} > 3\varepsilon$ distance away from q when ε is sufficiently small. This means the ball $B'' = B(q, 3\varepsilon)$ intersects the slab L_p within B. The ball B'' cannot have any sample point from L_p as B does not have any. Also, B'' cannot have any sample points from other slabs as B'' is contained in $B(p, 9\varepsilon)$ that has all sample points within L_p. A line passing through q and perpendicular to N_p must intersect the surface Σ within L_p since Σ separates these two planes within B'. Let this point be x. Then, $x \in \Sigma$ does not have any sample point within $3\varepsilon - 202\varepsilon^2 > \varepsilon$ distance violating the sampling condition (i). Therefore, the angle θ cannot be larger than 600ε as we assumed. □